INTRA BEAM SCATTERING IN LINEAR ACCELERATORS, ESPECIALLY ERLS

Georg H. Hoffstaetter, Michael P. Ehrlichman, Alexander B. Temnykh,
Cornell University, Ithaca, New York 14853

Abstract

The theories of beam loss and emittance growth by Touschek and Intra Beam Scattering have been formulated for beams in storage rings. It is there that these effects have hitherto been important because of their large currents. However, there are linear accelerators where these effects become important when considering loss rates and radiation damage. Prime examples are high current Energy Recovery Linacs (ERLs), managing these scattering effects can become challenging, and not only because of the large current, but also because the deceleration of the spent beam increases relative energy spread and transverse oscillation amplitudes. In this paper we describe two ways of simulating particle loss by these scattering affects, both implemented in Bmad. One that yields the places where scattering occurs, and another that yields loss rates along the chamber walls. Bmad includes nonlinear beam dynamics, wake effects, and more, which allows a rather complete propagation of scattered particle. For the example of the ERL x-ray facility that Cornell plans to build, we demonstrate that these capabilities are very important for designing a functional radiation protection system.

INTRODUCTION

Single event intra-beam scattering (IBS) that leads to momentum changes large enough to result in the loss of one or both of the colliding particles is called Touschek scattering, and particles that have been scattered to sufficiently large changes in momentum to be lost are called Touschek particles. Touschek scattering in a linear accelerator is interesting because the current of lost particles can pose a radiation hazard.

In this paper we describe tracking simulations developed to determine beam loss by Touschek scattering in a linear accelerator. The simulations determine the locations in a linear accelerator where Touschek particles are generated and where they are lost. Additionally, it determines the halo profile due to Touschek particles anywhere along the linac.

The development of these simulations was driven by Cornell ERL R&D [1]. The calculations shown in this paper used the Cornell ERL lattice version 3.0. The stages of the example accelerator are shown in table 1.
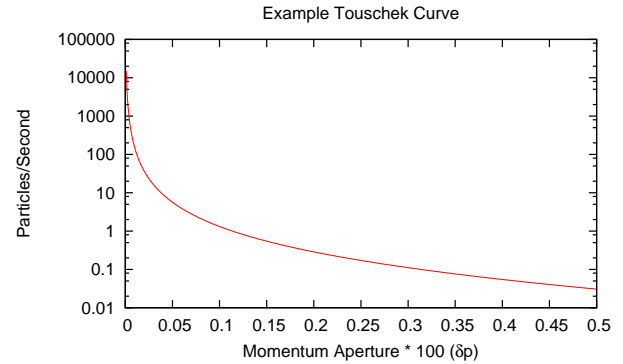

Figure 1: An example Touschek curve. Shown is the rate at which particles are kicked above δ_p versus δ_p.

THEORY

The theory behind our simulations is Piwinski's derivation of the Touschek effect [2]. Because of the broad range of energies encountered in a linear accelerator, we use the full, unapproximated, formula for the rate with which particles scatter beyond $p(1 + \delta_p)$,

$$R(\delta_p) = \frac{r_e^2 c \beta_x \beta_y \sigma_h N_b^2}{8\sqrt{\pi}\gamma^4\beta^2\sigma_{x\beta}^2\sigma_{y\beta}^2\sigma_z\sigma_p} \times \tag{1}$$

$$\int_{\tau_m}^{\infty} \left[\left(2 + \frac{1}{\tau}\right)^2 \left(\frac{\tau/\tau_m}{1+\tau} - 1\right) + 1 - \sqrt{\frac{1+\tau}{\tau/\tau_m}} \right.$$
$$\left. - \frac{1}{2\tau}\left(4 + \frac{1}{\tau}\right)\ln\frac{\tau/\tau_m}{1+\tau} \right] e^{-B_1\tau} I_0\left(B_2\tau\right) \sqrt{\frac{\tau}{1+\tau}} d\tau$$

where $\tau_m = \beta^2\delta_p^2$, and the remaining parameters are defined in [2]. An example plot for $R(\delta_p)$ is shown in shown in Fig. 1.

The momentum aperture of an element is the maximum relative momentum kick δ_p that can be introduced in an element without the particle colliding with the beam pipe or stopping further down the accelerator. The aperture is defined by a negative and positive bound, $[\delta_p^-, \delta_p^+]$.

In a ring the momentum aperture is typically considered to be the same for every element, and $\delta_p^- = -\delta_p^+$ is assumed.

However, the momentum aperture in a linear accelerator can vary significantly from one element to the next. The aperture has a strong dependence on energy and Twiss pa-

rameters. Due to asymmetries and nonlinearities the positive and negative bound are not symmetric. If the linac has decelerating sections then the Touschek particles that lose momentum can be stopped during deceleration. For example, a -0.3% momentum change at 5 GeV imparts a -15 MeV kick to the particle. If the beam is later decelerated to 10 MeV, the scattered particle will be stopped before reaching the end of the linac.

In a linac, the momentum aperture depends on where along the beam transport the scattering occurs. And the momentum aperture for energy gain can differ from that for energy loss as shown in Fig. 2. Because $R(\delta_p)$ describes the total number of scattered particles per time, $R(\delta_p^+)/2$ particles increase their energy beyond $(p + \delta_p^+)$, and $R(\delta_p^-)/2$ particles reduce their energy below $(p - \delta_p^-)$ per time.

Our simulations are developed within the general beam simulation library *Bmad* [3]. Standard *Bmad* subroutines provide lattice parsing and tracking. The tracking is fully nonlinear. The particle tracking portions of the simulations are parallelized with *PVM* [4].

IMPLEMENTATION

Overview

We begin when investigating Touschek scattering by determining the momentum aperture for each element in the accelerator. Then we construct a distribution of particles representing $R(\delta_p)$ outside the momentum aperture at each optical element and track these down the accelerator until they are lost.

Element-by-element momentum aperture

The positive and negative bounds of the momentum aperture are determined independently. In a low emittance linac, the physical aperture is much larger than the beam size, so one can assume to good approximation that scatteredparticles originate in the center of the beam. We determine δ_p^+ by a simple binary search for the smallest δ_p for which a particle is lost. Similarly δ_p^- is determined.

Generation of Touschek Particles

The number of Touschek particles generated per bunch passing for a given element is found by evaluating the production rate $R(\delta_p)$ using the Twiss and beam parameters at that element and multiplying by the time each bunch spends in the element. Repeating this calculation for all elements in a linac and multiplying by the charge per particle and the bunch repitition rate produces the Touschek generation profile.

An example is shown in Fig. 3.

Where Touschek particles are lost

To determine where the Touschek particles are lost, a distribution of test particles representative of $R(\delta_p)$ is pro-
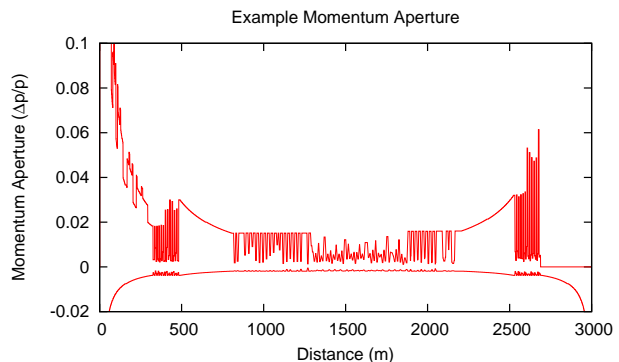

Figure 2: Example momentum aperture from CERL lattice version 3.0. The positive aperture is determined entirely by beam pipe collisions. The negative aperture is dominated by stopping during deceleration.
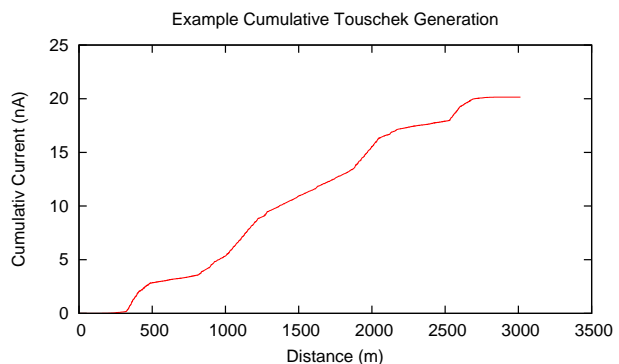

Figure 3: Integral over Touschek particle generation for CERL lattice version 3.0. $\epsilon_{nx,y} = 3.0 \times 10^{-7}$ m. Bunch charge is 77 nC and repitition rate is 1.3 GHz.

duced in the following way: The rate of scattering to above δ_p^+ is evaluated. Then this scattering rate is divided by the number of test particles we wish to track. We give each test particle equal weight so that each represents $\frac{R(\delta_p)}{N} \times \Delta t$ Touschek particles.

Determining the kick δ_p for each test particle requires

Table 1: Stages of CERL lattice version 3.0 used for example plots in this paper. Particles are injected at 0 m with 10 MeV.

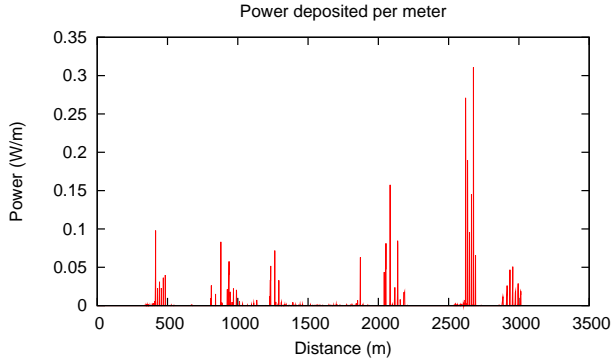| Start (m)	End (m)	Description
0	318	acceleration to 2.5 GeV
318	490	180 degree turn around, 43 meter radius
490	808	acceleration to 5.0 GeV
808	1284	wigglers, x-ray production
1284	1889	turn around through CESR
1889	2207	wigglers, x-ray production
2207	2525	deceleration to 2.5 GeV
2525	2696	180 degree turn around, 43 meter radius
2696	3014	deceleration to 10 MeV, then dump

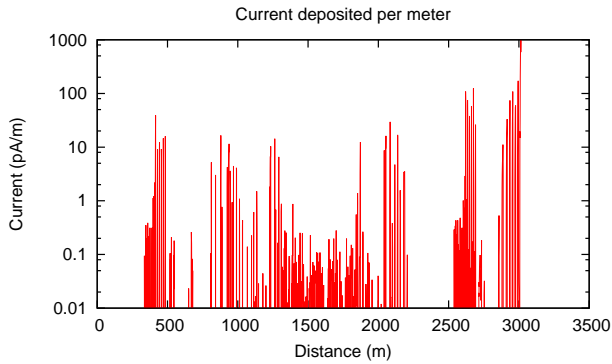Figure 4: Example plot of power deposited per meter.

Figure 5: Example plot of current deposited per meter.

inverting $R(\delta_p)$. This is done with a linear interpolation to obtain $\delta_p(R)$. The ith particle is generated with a momentum change of $\delta_p \left(\frac{R(\delta_p^+)}{N}(i - \frac{1}{2}) \right)$. Building the distribution in this manner guarantees that we have many test particles representing the interesting, high rate region, and fewer particles in the less interesting, low rate region.

Test particles representing the distribution of Touschek particles with $\delta_p < \delta_p^-$ are produced in a corresponding way, the ith one having $\delta_p = -\delta_p \left(\frac{R(\delta_p^-)}{N}(i - \frac{1}{2}) \right)$, representing $\frac{R(\delta_p^+)}{N} \times \Delta t$ Touschek particles.

The test particles are tracked from where they are created to where they are lost. Since the range of δ_p represented by the distribution is determined by the momentum aperture, it is guaranteed that each particle will be lost. Losses are due to either beam pipe collisions or stopping during deceleration. It is recorded where a particle is lost its energy and the momentum kick it suffered. From this data both the current and power deposited into each element can be calculated. The current deposited into each element is obtained by multiplying the rate at which scattered particles are deposited into the element by the charge per particle and the bunch repitition rate.

Shown in Figs. 4 and 5 are the power and current deposited per meter into the CERL lattice.

Collimation and beam dump considerations

Collimators are used to control where the beam pipe collisions occur. It is important to minimize the Touschek power in the user regions of an accelerator, and also around sensive equipment. The trajectories of the test particles are recorded, collimators are placed where ever the amplitude of scattered particles' trajectories are large. Collimation of intra-beam and residual gas scattered particles in the Cornell ERL has been studied in reference [5].

The halo of IBS particles around the beam at the end of the linac can impact the design of the dump. This halo can be studied by adjusting the simulation to track particles inside the momentum aperture of the machine, but outside one sigma of the beam dimensions.

CONCLUSION

The generation and behavior of Touschek particles in a linear accelerator can be simulated by adapting Piwinski's Touschek derivation. The results of these simulations can guide the placement of collimators to minimize radiation in the user areas and around other sensitive regions of an accelerator. The halo of scattered particles at the end of the linac can also be simulated and be taken into account in the design of beam dumps.

Acknowledgments

REFERENCES

[1] G.H. Hoffstaetter, *et. al.*, Challenges for Beams in an ERL Extension to CESR, EPAC2008 (2008)

[2] A. Piwinski, The Touschek Effect in Strong Focusing Storage Rings, DESY 98-179 (1998)

[3] D. Sagan, The Bmad Reference Manual, http://www.lns.cornell.edu/ dcs/bmad/ (2008)

[4] A. Geist, *et. al.* PVM: A Users' Guide, MIT Press (1994)

[5] A.B. Temnykh, Beam Losses Due to Intra-Beam And Residual Gas Scattering For Cornell's Energy Recovery Linac, EPAC2008 (2008)